

Linearization of a 500-W L-band GaN Doherty Power Amplifier by Dual-Pulse Trap Characterization

Tommaso Cappello¹, Corrado Florian², Alberto Santarelli², Zoya Popovic¹

¹ECEE Department, University of Colorado, USA

²DEI Department, University of Bologna, Italy

tommaso.cappello@colorado.edu

Abstract—This paper describes the linearization of a base-station L-band 500-W GaN Doherty high power amplifier (HPA) driven by OFDM signals. Pre-pulsing characterization is used to extract the gain dispersion of the carrier and peaking PAs due to trap-induced degradation of GaN-on-SiC transistors. Peak drain voltages reached by PA load-lines mainly set the trap states of the carrier and peaking PAs, while the recovery is longer with a dominant time constant of $100\ \mu\text{s}$ for this specific GaN technology. When the peak occurrences are below this dominant time constant of $100\ \mu\text{s}$, such as for symbol periods of 16.7 to $66.7\ \mu\text{s}$ (i.e., LTE/5G OFDM), the HPA trap-state remains approximately constant in the time interval between voltage peaks, allowing low-complexity linearization of the HPA. With a 10-MHz OFDM signal with peak-to-peak intervals shorter than $100\ \mu\text{s}$, a memory-less digital pre-distortion (DPD) is shown to improve ACLR by 4 dB and NRMSE by 1.6 percentage points, as compared to peak-to-peak intervals longer than $100\ \mu\text{s}$ when significant trap recovery takes place.

Keywords—characterization, current collapse, digital pre distortion (DPD), Doherty power amplifier, double pulse, Gallium Nitride (GaN), linearization, pre pulse, trapping effects

I. INTRODUCTION

Fifth generation (5G) communications orthogonal frequency division multiplexed (OFDM) standards use multiple carriers with sub-carrier spacing between 15 and 60 kHz, corresponding to 66.7 to $16.7\ \mu\text{s}$ symbol duration [1]. The greater than 100 MHz bandwidth contains thousands of carriers, giving rise to signals with high peak-to-average power ratios (PAPRs). The transmitter power amplifier (PA) needs to linearly amplify such signals, consuming as little power as possible. The Doherty PA has been the architecture of choice for basestation PAs for maintaining efficiency in backoff, and usually requires digital predistortion (DPD) to meet linearity requirements.

Current L-band basestation PAs use LDMOS devices, but GaN is emerging as the technology of choice for high-power amplifiers (HPAs) due to its high voltage operation, high cutoff frequencies, and impedances that enable broadband matching. In a GaN HEMT, charge trapping results in dynamic modulation of the transistor I - V characteristics, known as current collapse, knee walkout, and kink effect [2], [3]. Experimental evidence has shown that the trapping state is mainly set by a combination of the intrinsic gate and drain peak voltages in the transistor which activates fast charge capture in the trap states, while the release is typically slower, with time constants in the order of tenth of μs to ms [4], [5]. This device-level degradation translates into modification of

the small- and large-signal characteristics of a transistor [6], [7], [8] and affects PA architectures such as the Doherty.

In this paper, we analyze the trap-induced degradation of a 500-W L-band GaN Doherty HPA for base-station transmitters. First, a dual-pulse characterization of the HPA is performed to investigate the gain degradation in the second (measurement) pulse caused by the first (pre-pulse) peak voltage, and extract the associated gain-recovery time constant. Then, OFDM signals are used to verify the gain degradation with a “multi-pulse” drive of the HPA. Finally, the approach is validated by showing how the different peak-to-peak time-domain separations impact the linearization of the HPA.

II. GAN DOHERTY HPA AND MEASUREMENT SETUP

A hybrid Doherty HPA, shown in Fig. 1, with devices fabricated in a $0.25\text{-}\mu\text{m}$ GaN-on-SiC process and designed for downlink base-station transmitters is studied in terms of linearity with modulated signals. The HPA is based on two, co-packaged carrier and peaking PAs, and is designed to operate at L-band (1.805-1.88 GHz) with back-off efficiency optimized at -6 dB peak output power. The HPA is a typical Doherty design with class-AB bias on the carrier and class-C on the peaking PA.

The HPA is tested with a 200-MHz bandwidth vector signal transceiver (NI VST 5646R) which allows the generation and analysis of modulated signals up to 6 GHz with 16-bit resolution. The RF output of the VST is amplified by a driver amplifier (AR 60S1G3) which provides up to 44 dBm

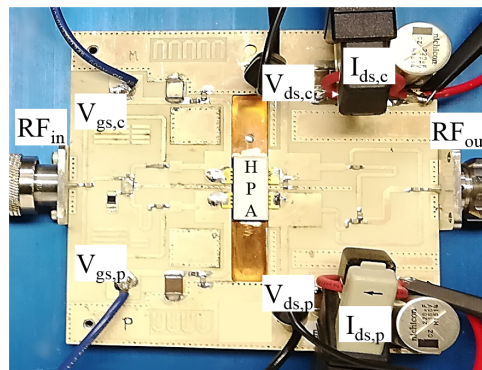


Fig. 1. Photo of the 500-W L-band GaN base-station Doherty HPA with indicated RF input, output, and biasing. Separate voltage and current sensing is performed on the carrier and peaking amplifiers.

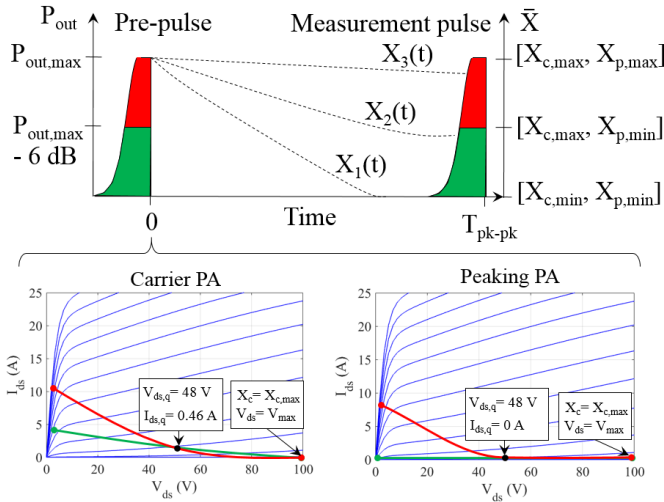


Fig. 2. Pulse regime used to study the HPA trap-induced performance degradation. The pre-pulse amplitude is used to set the HPA trap-state, and the associated performance degradation is extracted by the following measurement pulse. \bar{X} designates the trap state, and the peak-to-peak time T_{pk-pk} between the two pulses is varied to measure the trap recovery time.

input power to the HPA with less than 0.05 dB compression and with a gain of 51.7 dB. The output of the HPA is attenuated by using N-type attenuators. Scalar calibration is performed at the input and output port of the HPA. The bias currents of the carrier and peaking PAs are provided by two isolated voltage supplies (Agilent 6654A) which are sensed separately with ac-dc current probes (Tek TCP0030).

III. HPA CHARACTERIZATION

The gain characteristics of the Doherty HPA are studied as a function of an architecture-level trap-state $\bar{X} = [X_c, X_p]$, in which X_c and X_p are the individual trap-state of the carrier and peaking PA, respectively. The characterization sequence is shown in Fig. 2. A pre-pulse of 1- μ s duration sets the HPA trap-state \bar{X} to a pre-selected level. For example, at the peak output power $P_{out,max}$, both PA load-lines reach the maximum drain-source voltage, hence the corresponding HPA trap-state is set to $\bar{X}_{max} = [X_{c,max}, X_{p,max}]$ [5], [6], [7]. On the other hand, when only the quiescent bias of the transistor is present, the HPA trapping-state is at the minimum, $\bar{X}_{min} = [X_{c,min}, X_{p,min}]$. For the considered Doherty HPA, at 6-dB output power back-off only the carrier PA is active and saturated, and the corresponding HPA trap-state is $[X_{c,max}, X_{p,min}]$. After the pre-pulse, a measurement pulse of 1- μ s duration with half-Gaussian amplitude modulation is used to extract the HPA characteristics. The characterization is performed with short pulses and duty cycle below 1% to minimize HPA self-heating due to signal amplification and extract only the trap-related behavior.

A variable delay, T_{pk-pk} , between the two pulses is used to measure the PA characteristic variations associated with the trapped charge recovery. We indicate with τ_1 the dominant time constant of the recovery mechanism from the maximum trapping state \bar{X}_{max} (i.e., at $P_{out,max}$) to a certain degree of

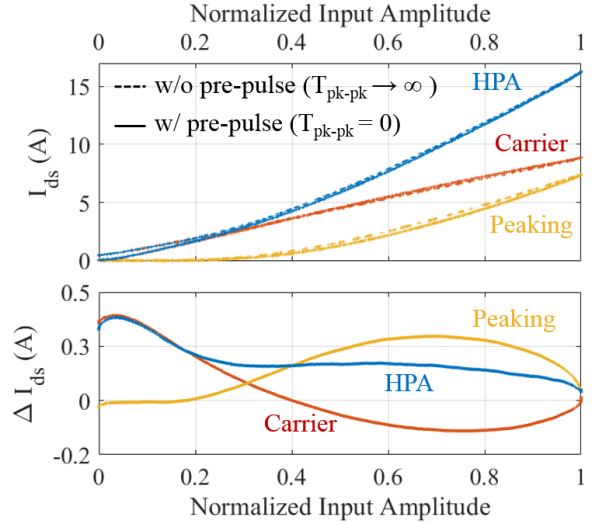


Fig. 3. Drain current I_{ds} of the carrier, peaking, and Doherty HPA, with and without pre-pulse (top figure) and associated current variation ΔI_{ds} (bottom figure). ΔI_{ds} shows how the peak voltages impact differently the carrier and the peaking PAs because of load modulation and different operation classes.

recovery of the trap-state $\bar{X}(t)$. With reference to Fig. 2, three different scenarios are possible: (1) $\bar{X}_1(t)$ recovers completely before the next measurement pulse ($T_{pk-pk} \gg \tau_1$); (2) $\bar{X}_2(t)$ recovers partially ($T_{pk-pk} \approx \tau_1$); and (3) the trap-state $\bar{X}_3(t)$ remains fixed at the maximum value for the carrier and peaking PAs, respectively.

IV. HPA MEASUREMENT RESULTS

With this characterization technique, trap-induced degradation of the Doherty HPA is evaluated first as a function of the pre-pulse power and then as a function of the peak-to-peak interval T_{pk-pk} when the maximum pre-pulse power is used.

Fig. 3 shows the drain current, without ($T_{pk-pk} \rightarrow \infty$) and with pre-pulse (case $T_{pk-pk} = 0$), and the associated current reduction ΔI_{ds} when a pre-pulse is used, which can be associated to the trap-induced current collapse in the GaN HEMTs [2], [5], [6]. At low input amplitudes, current reduction is present only on the carrier PA whereas at higher amplitudes the peaking PA shows a similar effect. Interestingly, at higher amplitudes the carrier PA shows an “inverted” current collapse which can be interpreted as an interaction of the two PAs through load-modulation¹, similarly to what is shown in [8]. The total current variation $\Delta I_{ds,tot}$ of the HPA is however positive over the whole output range.

Fig. 4(a) reports the gain variation for different pre-pulse powers ($T_{pk-pk} = 0$), and the normalized current reduction $\Delta I_{ds,tot}$ of the HPA at $P_{out,max}$. Without a pre-pulse, the gain shows the typical Doherty “hump”, with a value of about 16 dB at small-signal, and 13 dB at $P_{out,max} = 57.1$ dBm (512 W). When a pre-pulse is used, the small-signal gain drops

¹From [9], the load impedance of the carrier PA when the peaking PA turns on is $Z_{l,c} = R_l(1 + I_{ds,p}/I_{ds,c})$ which highlights the interaction between the two current generators, $I_{ds,p}$ and $I_{ds,c}$, through load modulation.

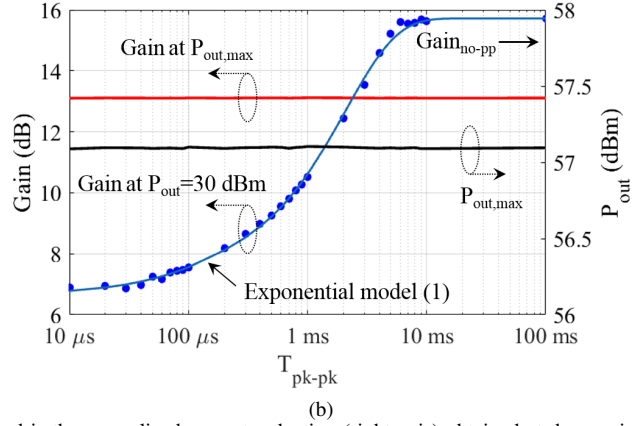
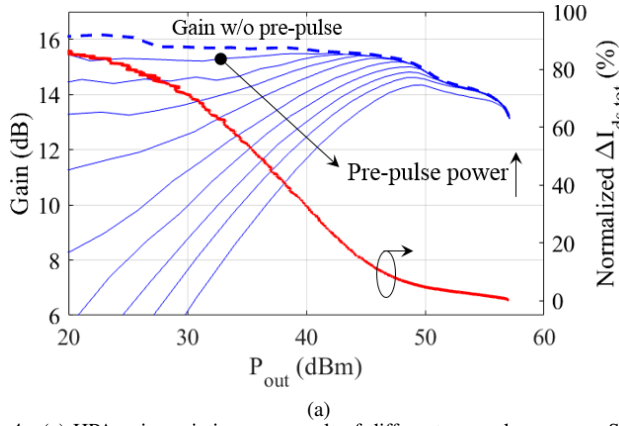


Fig. 4. (a) HPA gain variation as a result of different pre-pulse powers. Superposed is the normalized current reduction (right axis) obtained at the maximum pre-pulse power. (b) Measured HPA gain and output power variation for different peak-to-peak intervals (T_{pk-pk}). The gain at 30dBm output presents a significant gain collapse for $T_{pk-pk} < 6$ ms, whereas the peak output power $P_{out,max}$ and the corresponding gain is not affected by the pre-pulse.

considerably due to current collapse in the HEMTs of the carrier amplifier. When the peaking PA turns on, the gain is extended to reach the maximum output power and the gain variation is less consistent in agreement with the negligible current-collapse variation (less than 10%).

Next, the gain and output power are evaluated as a function of the peak-to-peak interval T_{pk-pk} , and the measured results are reported in Fig. 4(b). An exponential model for the gain

$$G = G_{no-pp} + \sum_{i=0}^N a_i e^{-\frac{T_{pk-pk}}{\tau_i}}, \quad (1)$$

is fitted to the experimental data to find the trap-recovery time constants [10]. Here, the asymptotic gain is $G_{no-pp} = 15.7$ dB ($T_{pk-pk} \rightarrow \infty$) and the two time constants are: $\tau_1 \approx 100$ μ s ($a_1 = -0.8$ dB) and $\tau_2 \approx 2.1$ ms ($a_2 = -8.3$ dB). Therefore, for $T_{pk-pk} < \tau_1$ no significant gain recovery is expected since the trap-state of the HPA is practically fixed at \bar{X}_{max} . Note that all the symbol durations considered in 5G OFDM fall in this interval, the longest one being 66.7 μ s [1]. After 100 μ s and up to 6 ms the HPA recovers towards its “un-trapped” characteristics.

Now, in place of narrow-band Gaussian pulses, OFDM signals with high PAPR are considered, which are generated with the algorithm of [11]. Fig. 5 depicts the typical envelope of an OFDM symbol which is here used to validate the characteristics of Fig. 4. Similarly to the sequence of Fig. 2, in this “multi-pulse” signal the first peak at the maximum power acts as a “pre-pulse” and, after a time T_{pk-pk} , the second peak acts as the “measurement pulse” which is used to extract the HPA characteristics (i.e., the HPA behavior over its entire dynamic range swept by the signal peak). With this sequence, the dynamic gain for four T_{pk-pk} durations with the same peak power levels are obtained and shown in Fig. 6. For $T_{pk-pk} = 67$ μ s, the gain tends to overlap with the narrow-band measurement of Fig. 4(a). For longer T_{pk-pk} , the back-off gain becomes more scattered. Interestingly, for $T_{pk-pk} = 0.67$ ms and 1.33 ms the combination of secondary peak powers and trap recovery time generates two overlapping

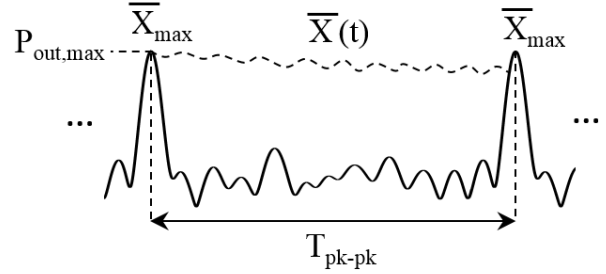


Fig. 5. Schematic representation of an OFDM envelope with two peaks separated by T_{pk-pk} . If T_{pk-pk} is shorter than the τ_1 recovery time, the HPA trap state $\bar{X}(t)$ remains fixed at \bar{X}_{max} , which is determined by the peak voltages ($P_{out,max}$).

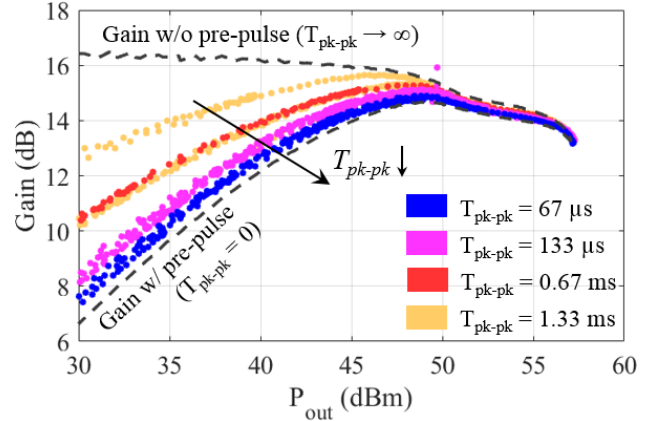


Fig. 6. Dynamic gain for different T_{pk-pk} intervals (67 μ s, 133 μ s, 0.67 ms, and 1.33 ms) with a modulated signal of 10-dB PAPR and 10-MHz bandwidth. As T_{pk-pk} increases, the gain tends to recover to the static gain characterization obtained without pre-pulse.

gains in back-off. In summary, the gain variation with modulated signals is more evident outside the Doherty region, in agreement with the results of Fig. 4(a).

Finally, the HPA is tested with DPD extracted with two sequences, one with peak-to-peak duration of 67 μ s (i.e., $\Delta f = 15$ kHz) and the other with 1.33 ms. A memory-less polynomial of the 13th order is used for both DPDs and two iterations are performed to extract the coefficients. In the

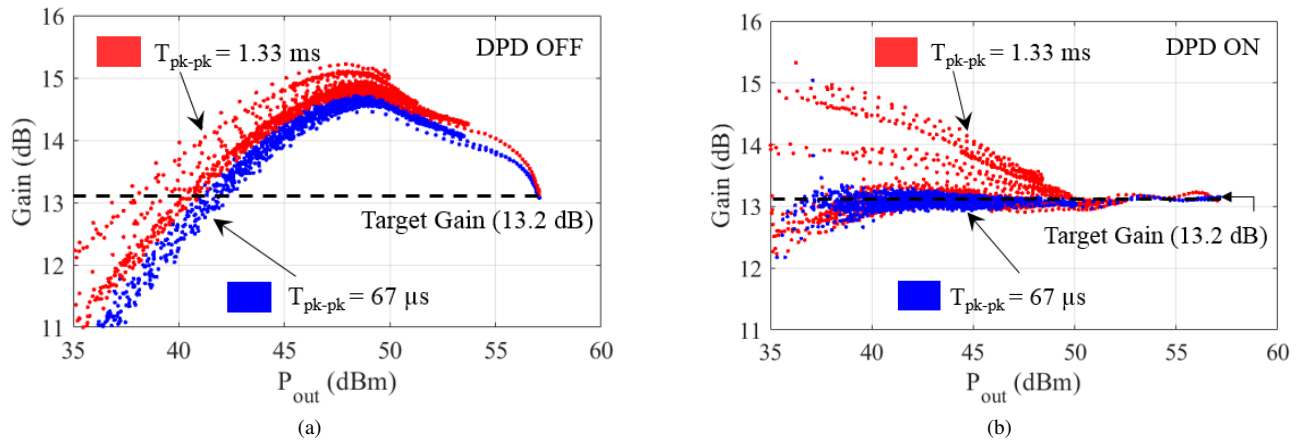


Fig. 7. (a) HPA gain dispersion without DPD for 67- μ s and 1.33-ms peak-to-peak intervals. Higher dispersion due to multiple time constants are evident in the 1.33-ms case. (b) When the memory-less DPD is applied on the 67- μ s sequence, the DPD provides a better linearization as compared to the 1.33 ms whereas some gain recovery is visible in backoff.

case without DPD, Fig. 7(a), significant dispersion is evident due to the modulation of the gain characteristics performed by different time constants, whereas for $T_{pk-pk} \leq 66.7 \mu$ s the dispersion is less pronounced. The DPD compensation, Fig. 7(b), is more effective with the shortest peak-to-peak duration, especially outside the Doherty region where only the carrier PA is active. This is the result of using a $T_{pk-pk} \leq \tau_1$ for which the HPA trap-state is fixed, $\bar{X} \approx \bar{X}_{max}$. It is worth observing that the typical sub-carrier spacings of 5G are all below the dominant trap release time constant $\tau_1 \approx 100 \mu$ s.

Fig. 8 shows the output power spectra of a 10-MHz, 10-dB PAPR OFDM signal without DPD and with DPD extracted with one sequence and with peak-to-peak intervals of 67 μ s and the other with 1.33 ms. With the shorter T_{pk-pk} , ACLR varies from -46.5 dB to -50.6 dB (4.1 dB improvement), while the NRMSE calculated between the transmitted and received symbol improves from 2.8% to 1.2% (1.6 point improvement).

These results indicate that if the typical peak occurrence of the signal is short compared to the GaN technology trap recovery time, the dual-pulse technique can be used to identify a simple effective DPD that demonstrates suitable performance. This is in accordance with similar behaviors shown in [5] for a different GaN technology. Further research with longer transmission sequences (i.e., an OFDM frame) is under way, and significant self-heating and interaction with the trap-states in the HPA is expected for tens of milliseconds long sequences.

REFERENCES

- [1] S. Lien, S. Shieh, Y. Huang, B. Su, Y. Hsu, and H. Wei, "5g new radio: Waveform, frame structure, multiple access, and initial access," *IEEE Commun. Mag.*, vol. 55, no. 6, pp. 64–71, June 2017.
- [2] G. P. Gibiino, C. Florian, A. Santarelli, T. Cappello, and Z. Popovic, "Isotrap pulsed *iv* characterization of gan hemts for pa design," *IEEE Microw. Wireless Compon. Lett.*, vol. 28, no. 8, pp. 672–674, Aug 2018.
- [3] O. Jardel, F. D. Groote, T. Reveyrand, J. Jacquet, C. Charbonniaud, J. Teyssier, D. Floriot, and R. Quere, "An electrothermal model for algan/gan power hemts including trapping effects to improve large-signal simulation results on high vswr," *IEEE Trans. Microw. Theory Techn.*, vol. 55, no. 12, pp. 2660–2669, Dec 2007.
- [4] A. Santarelli, R. Cignani, G. P. Gibiino, D. Niessen, P. A. Travesso, C. Florian, D. M. M. Schreurs, and F. Filicori, "A double-pulse technique for the dynamic *i/v* characterization of gan fets," *IEEE Microw. Wireless Compon. Lett.*, vol. 24, no. 2, pp. 132–134, Feb 2014.
- [5] C. Florian, T. Cappello, A. Santarelli, D. Niessen, F. Filicori, and Z. Popovic, "A prepulsing technique for the characterization of gan power amplifiers with dynamic supply under controlled thermal and trapping states," *IEEE Trans. Microw. Theory Techn.*, vol. 65, no. 12, pp. 5046–5062, Dec 2017.
- [6] A. Raffo, G. Avolio, V. Vadal, G. Bosi, G. Vannini, and D. Schreurs, "Assessing gan fet performance degradation in power amplifiers for pulsed radar systems," *IEEE Microw. Wireless Compon. Lett.*, vol. 28, no. 11, pp. 1035–1037, Nov 2018.
- [7] L. C. Nunes, J. L. Gomes, P. M. Cabral, and J. C. Pedro, "A simple method to extract trapping time constants of gan hemts," in *2018 IEEE/MTT-S Int. Micr. Symp. - IMS*, June 2018, pp. 716–719.
- [8] L. C. Nunes, P. M. Cabral, and J. C. Pedro, "Impact of trapping effects on gan hemt based doherty pa load-pull ratios," in *2015 Integr. Nonlin. Microw. Mm-wave Circ. Workshop (INMMiC)*, Oct 2015, pp. 1–3.
- [9] S. C.ripps, *RF Power Amplifiers for Wireless Communications*, 2nd ed. 685 Canton Street Norwood, MA 02062, USA: Artech House, 2006.
- [10] J. Joh and J. A. del Alamo, "A current-transient methodology for trap analysis for gan high electron mobility transistors," *IEEE Trans. Electron Devices*, vol. 58, no. 1, pp. 132–140, Jan 2011.
- [11] T. Cappello, A. Duh, T. W. Barton, and Z. Popovic, "A dual-band dual-output power amplifier for carrier aggregation," *IEEE Trans. Microw. Theory Techn.*, pp. 1–13, 2019.

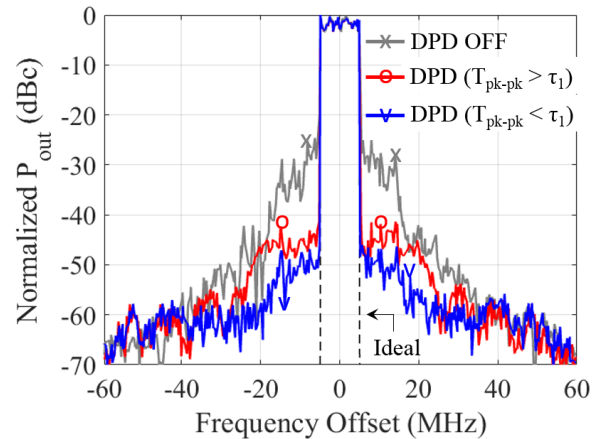


Fig. 8. Output spectra of a 10-MHz, 10-dB PAPR OFDM signal without DPD, and with DPD with peak-to-peak interval higher and shorter than the dominant trap-recovery time constant ($\tau_1 = 100 \mu$ s). No memory correction is used in DPD.